

Influence of sintering on electrical properties and phase transition of $\text{La}_2\text{Mo}_2\text{O}_9$

R. A. Rocha, E. N. S. Muccillo

Multidisciplinary Center for the Development of Ceramic Materials
Energy and Nuclear Research Institute– IPEN - CCTM
CP 11049 CEP 05422-970 S. Paulo – SP – Brazil
enavarro@usp.br

Keywords: phase transition, sintering, differential thermal analysis, electrical properties

Abstract: High ionic conductivity ceramics have potential technological applications in chemical sensors, ceramic permeable membranes, oxygen pumps, and solid oxide fuel cells. Recently ionic conductivity values as high as those of doped zirconia solid solutions have been found in a lanthanum molybdate compound. The high ionic conductivity of this compound, $\text{La}_2\text{Mo}_2\text{O}_9$, is obtained at temperatures above the structural phase transition temperature (~ 580 °C). In this work the $\text{La}_2\text{Mo}_2\text{O}_9$ ceramic material was prepared by the polymeric precursor technique and sintered at several dwell temperatures and soaking times to study the effect of sintering conditions on phase transition. It was found that there is a strong dependence of phase transition on the sintering profile. At 950 °C the phase transition is suppressed for short soaking times, whereas it is observed to occur for longer times. Moreover, the relative magnitude of conductivity is also dependent on the sintering conditions. The main conclusion is that the phase transition in $\text{La}_2\text{Mo}_2\text{O}_9$ is particle size-dependent.

Introduction

The $\text{La}_2\text{Mo}_2\text{O}_9$ compound is one of the most recent oxide ion conductors that have been reported [1]. This compound crystallizes with a different structure than the well-known fluorite, perovskite and pyrochlore oxide ion conductors [2,3]. The phase diagram of La_2O_3 - MoO_3 system is known since 1970. However, the high ionic conductivity of this phase was discovered only recently [1,4].

The $\text{La}_2\text{Mo}_2\text{O}_9$ compound exhibits a structural phase transition at approximately 580 °C, from the low-symmetry α -phase to a cubic β -phase [5]. This phase transition has been shown to be of first order, reversible and with a hysteresis on heating and cooling of the samples [1,6-8]. In addition, the ionic conductivity of the high-temperature β -phase is almost 2 orders of magnitude higher than that of the low-symmetry phase.

Some characterization techniques such as differential thermal analysis, X-ray diffraction, internal friction and impedance spectroscopy have been used to study the phase transition or the stabilization of β - $\text{La}_2\text{Mo}_2\text{O}_9$ phase at room temperature [1,5,8,9].

In most of these studies, solid state synthesis methods were used. It is generally known that chemical methods, both solution or gas phase methods, allow for better control of homogeneity and stoichiometry compared to solid state synthesis methods. Relatively few works may be found in the literature where a chemical method was used for the synthesis of the $\text{La}_2\text{Mo}_2\text{O}_9$ compound [10-16].

In this work, the $\text{La}_2\text{Mo}_2\text{O}_9$ compound was prepared by the polymeric precursor technique based on the Pechini method [17] to study the influence of sintering parameters on densification, on phase transition and on the electrical properties of this compound.

Experimental

La_2O_3 (IPEN, 99.9%), MoO_3 (Alfa Aesar, 99%), anhydrous citric acid and ethylene glycol, both analytical grade, were used as starting materials. In this synthesis, a metal : acid citric 1:2 molar ratio and a citric acid : ethylene glycol 60:40 mass ratio were utilized. A full account on the synthesis method may be found elsewhere [14]. The obtained resin was first pyrolyzed at 200 °C for 1 h and then calcined at 550 °C for 3 h. Pellets of about 10 mm diameter were prepared by uniaxial pressing at 96 MPa and sintered without any previous mechanical treatment. The sintering was carried out at 950 or 1000 °C dwell temperatures for 3, 24 or 96 h soaking times, with powder bed of the same composition.

The X-ray diffraction, XRD (D8 Advance, Bruker-AXS) method was used for phase analysis. The equipment has a Ni-filtered Cu K_α radiation source and the experimental conditions were 40 kV, 40 mA, with scans at 15-75° 2θ range at 0.05° per 10 s counting time. The fracture surface of sintered pellets were observed by scanning electron microscopy (XL 30, Philips), using secondary electrons. The apparent densities were measured by geometric and immersion methods.

The phase transition was studied by differential thermal analysis, DTA (STA 409, Netzsch) from room temperature up to 700 °C, with heating and cooling rates of 20 and 15 °C min^{-1} , respectively, in a dynamic atmosphere of synthetic air, using $\alpha\text{-Al}_2\text{O}_3$ (Alcoa) as reference. Electrical conductivity measurements by impedance spectroscopy (HP 4192A) technique were also used to study the phase transition. Resistance measurements were carried out during heating of the samples from 400 to 600°C.

Results and discussion

Fig. 1 shows X-ray diffraction patterns of the $\text{La}_2\text{Mo}_2\text{O}_9$ compound sintered at different temperatures and times. It can be seen in these XRD patterns that most of the high-intensity XRD peaks correspond to those of the $\beta\text{-La}_2\text{Mo}_2\text{O}_9$ phase. However, some extra diffraction peaks can also be observed, and they are probably related to the $\alpha\text{-La}_2\text{Mo}_2\text{O}_9$ phase. The difference in the angular position of the main diffraction peaks in α - and β - phases is due to slight displacements of atoms, and they can be identified, with no ambiguity, only by using high resolution techniques [5].

Table 1 shows apparent density values of studied samples. The sample sintered at 950°C for 3 h has a low density value. For other sintering conditions high values (> 94% of the theoretical value) of sintered density were obtained. Increasing of the soaking time from 3 to 24 h at 950 °C resulted in an increase of the apparent density. In contrast, a further increase in the soaking time to 96 h produces a decrease of the sintered density. For a fixed soaking time of 3 h, the increase in the dwell temperature from 950 to 1000 °C also induces an increase of the sintered density. These results are similar to those obtained for specimens prepared by the freeze drying method [15,16].

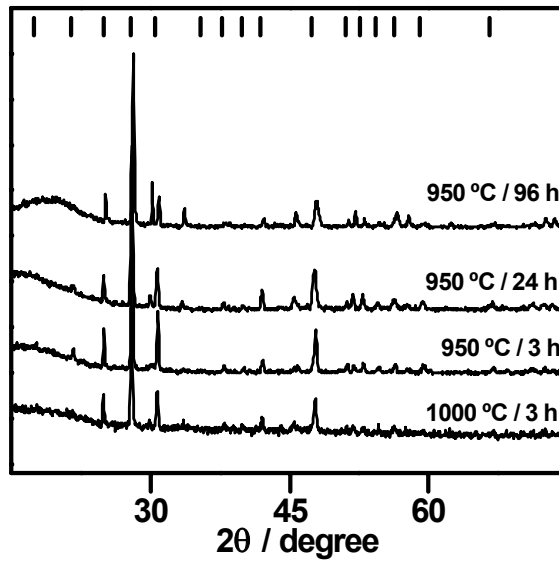


Figure 1. XRD patterns of samples sintered under different conditions. | corresponds to β - $\text{La}_2\text{Mo}_2\text{O}_9$ (ICDD 28-0509).

Table 1. Values of green (d) and sintered (geometric – d_g , hydrostatic d_h , and theoretical d_t) density of compacts.

Sintering ($^{\circ}\text{C} / \text{h}$)	d ($\text{g}\cdot\text{cm}^{-3}$)	d_g ($\text{g}\cdot\text{cm}^{-3}$)	d_h/d_t (%)
950 / 24	2.10 ± 0.1	4.97 ± 0.2	97.2
950 / 96	2.10 ± 0.1	4.76 ± 0.1	94.1
950 / 3	2.07 ± 0.1	4.82 ± 0.2	85.6
1000 / 3	2.14 ± 0.1	5.01 ± 0.1	95.4

Fig 2 shows SEM micrographs of fracture surfaces of the sintered samples. The morphology of pores and grains is different, showing a direct relationship with sintering time and temperature. The micrograph of the specimen sintered at 950 $^{\circ}\text{C}$ for 3 h reveals extensive porosity and regions with different degree of densification. However, after sintering at 1000 $^{\circ}\text{C}$ for 3 h, the micrograph shows grains with larger grain size than that sintered at 950 $^{\circ}\text{C}$ for 3 h and a small fraction of porosity. The same can be observed on the micrographs of pellets sintered at 950 $^{\circ}\text{C}$ for 24 or 96 h. With increasing of the soaking time from 24 to 96 h, at 950 $^{\circ}\text{C}$, the changes on the morphology of fracture surface are not significant, although this parameter has influenced the final density, as shown in table 1.

Fig. 3 shows results of the $\alpha \leftrightarrow \beta$ phase transition measured by differential thermal analysis. The phase transition shows a characteristic endothermic peak during heating and a corresponding exothermic peak on cooling down the sample. The peak temperature of thermal events is different on heating and cooling evidencing the hysteresis typical of a first order transition. These results show that $\text{La}_2\text{Mo}_2\text{O}_9$ has a reversible first order phase transition in agreement with previous observations [1,5,8,15,18].

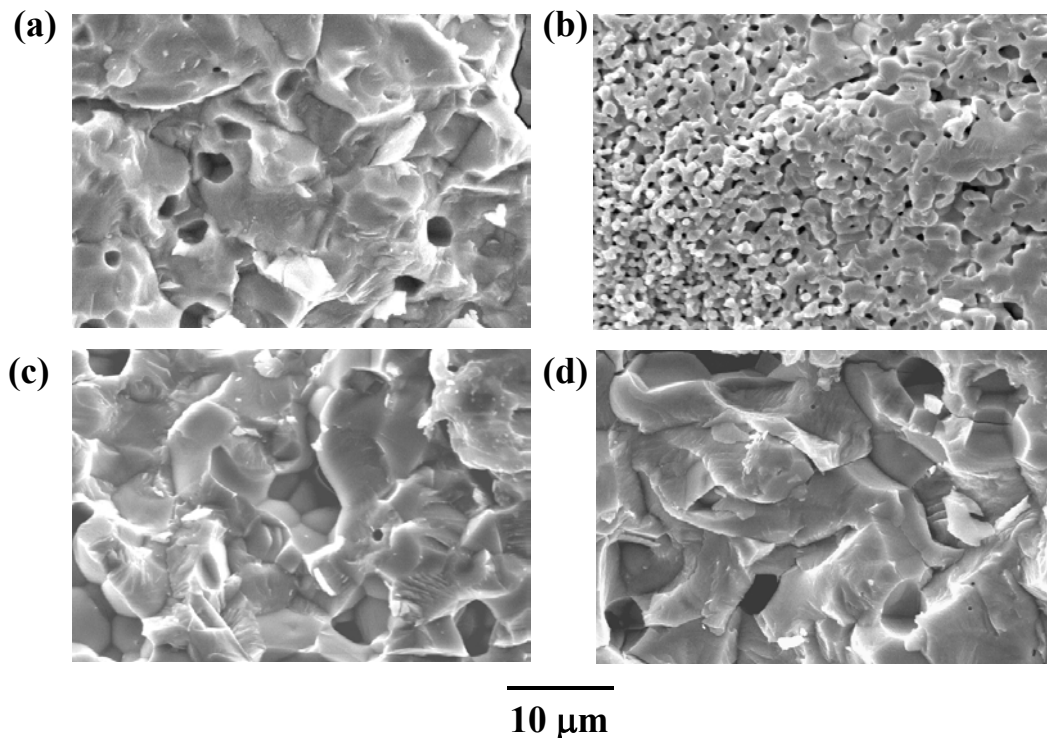


Figure 2. SEM micrographs of fractured surfaces of pellets sintered at (a) 1000 °C / 3 h, (b) 950 °C / 3 h, (c) 950 °C / 24 h and (d) 950 °C / 96 h.

Specimens sintered at 950 °C for 3 h do not exhibit the reversible phase transition. Moreover, the temperature range where the phase transition occurs is dependent on the sintering conditions. The overall results may be explained based on the small size of the particles prepared by this method and the grain size attained after sintering. It may be concluded that the phase transition in $\text{La}_2\text{Mo}_2\text{O}_9$ is suppressed in specimens with small grain size and, therefore, it is particle size-dependent.

Electrical conductivity measurements were carried out to determine the temperature range of phase transition. Fig. 4 shows the Arrhenius plot of the electrical conductivity of studied samples. The specimen sintered at 950 °C for 3 h does not present any change in the slope, meaning that no phase transition occurs at that temperature range. This result corroborates that of thermal analysis. It is important to note that the electrical conductivity of this sample is lower than that of other samples in the whole temperature range of measurements.

Samples sintered at 1000 °C for 3 h, 950 °C for 24 h and 950 °C for 96 h exhibit an abrupt change in the order of magnitude of the electrical conductivity due to the phase transition. These samples have similar conductivity values in high temperature regime.

The ratio between the high- and low-temperature conductivity is similar in all samples presenting the phase transition. In $\text{La}_2\text{Mo}_2\text{O}_9$ prepared by chemical techniques, the total conductivity is dependent on the microstructure, as well as the phase transition [14,15]. The

temperature range of phase transition derived from thermal analysis or electrical conductivity is similar for sample sintered at the same conditions.

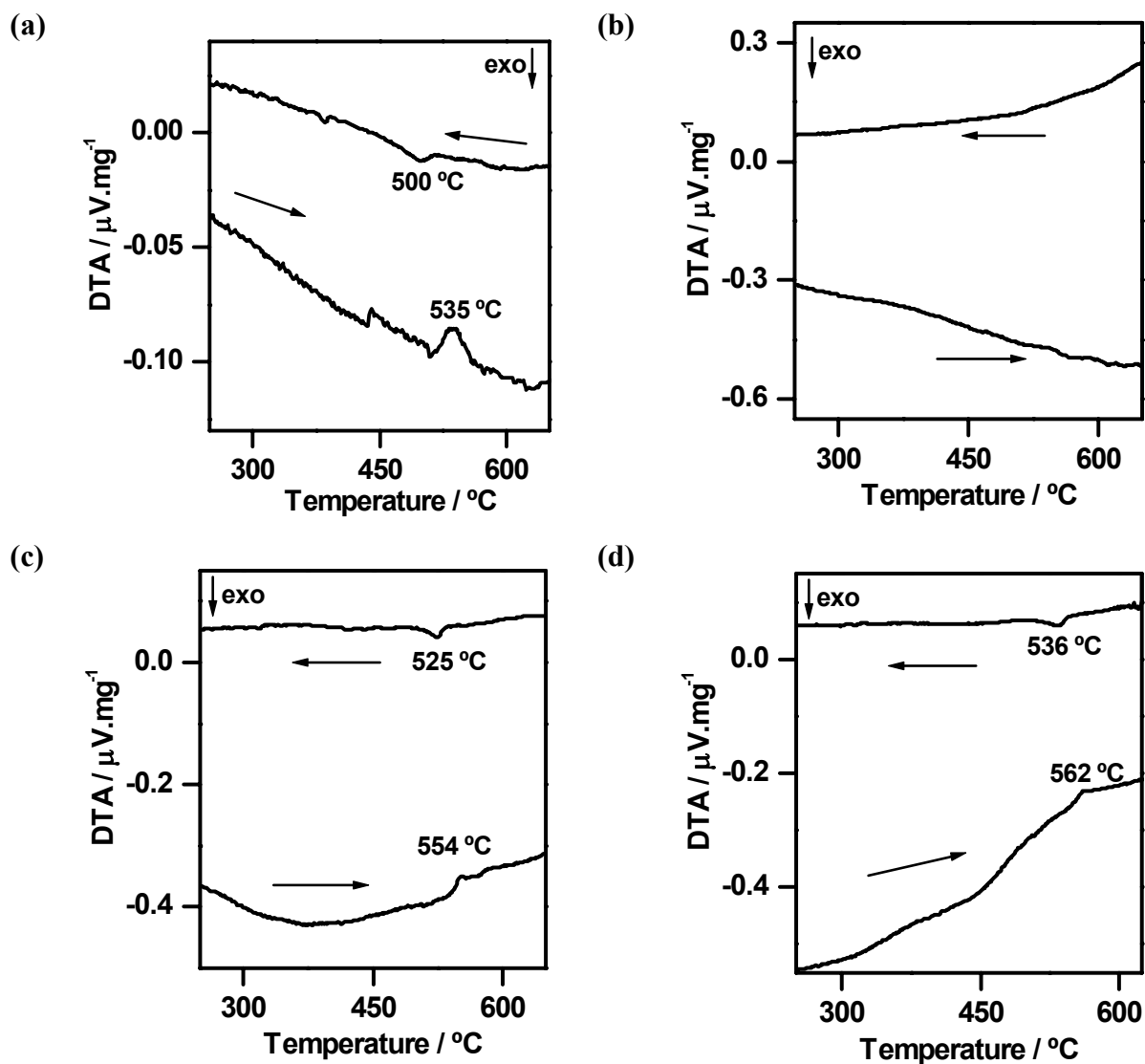


Figure 3. DTA results of samples sintered at (a) 1000 $^{\circ}\text{C}$ / 3 h, (b) 950 $^{\circ}\text{C}$ / 3h, (c) 950 $^{\circ}\text{C}$ / 24 h and (d) 950 $^{\circ}\text{C}$ / 96 h.

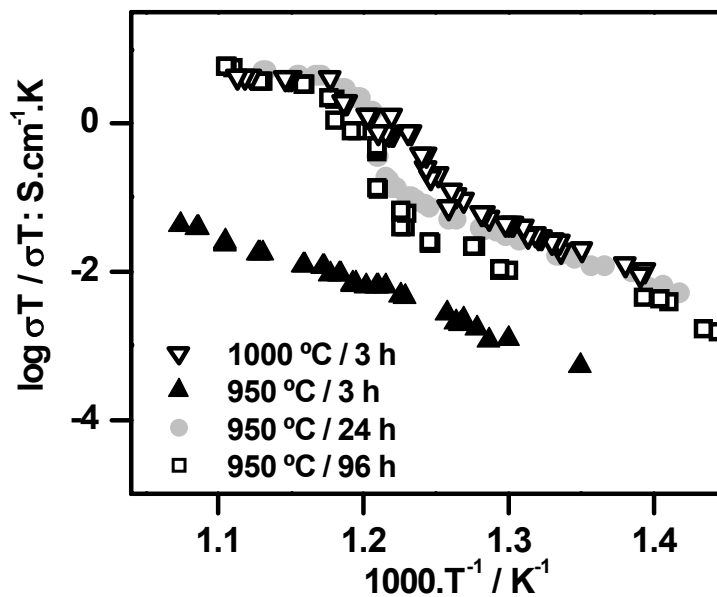


Figure 4. Arrhenius plots of the electrical conductivity of sintered samples.

Conclusions

High density pellets of $\text{La}_2\text{Mo}_2\text{O}_9$ were obtained by sintering at $950\text{ }^\circ\text{C} / 24\text{ h}$. The $\alpha \leftrightarrow \beta$ phase transition is suppressed in specimens with small grain sizes as shown by thermal analysis and electrical conductivity. Increasing the sintering temperature or time does not change the ionic conductivity of $\text{La}_2\text{Mo}_2\text{O}_9$ for samples with large grain sizes.

Acknowledgements

The authors acknowledge FAPESP, CNPq and CNEN / IPEN for financial support. R. A. Rocha acknowledges FAPESP (01/12269-7) for the scholarship.

References

- [1] P. Lacorre, F. Goutenoire, O. Bohnke, R. Retoux, Y. Lalignant, *Nature* **404** (2000) p. 856.
- [2] J. B. Goodenough, *Annual Review Materials Research* **33** (2003) p. 91.
- [3] D. Z. de Florio, F. C. Fonseca, E. N. S. Muccillo, R. Muccillo, *Cerâmica* **50** (2004) p. 275.
- [4] J. P. Fournier, J. Fournier, R. Kohlmuller, *Bull. Soc. Chim. Fr.* **12** (1970) p. 4277.
- [5] F. Goutenoire, O. Isnard, R. Retoux, P. Lacorre, *Chem. Mater.* **12** (2000) p. 2575.
- [6] D. S. Tsai, M. J. Hsieh, J. C. Tseng, H. S. Lee, *J. Eur. Ceram. Soc.* **25** (2005) p. 481.
- [7] S. Georges, F. Goutenoire, F. Altorfer, D. Sheptyakov, F. Fauth, E. Suard, P. Lacorre, *Solid State Ionics* **161** (2003) p. 231.
- [8] S. A. Hayard, S. A. T. Redfern, *J. Phys.: Condens. Matter* **16** (2004) p. 3571.
- [9] X. P. Wang, Q. F. Fang, *J. Phys.: Condens. Matter* **13** (2001) p. 1641.
- [10] W. Kuang, Y. Fan, K. Yao, Y. Chen, *J. Solid State Chem.* **140** (1998) p. 354.
- [11] R. A. Rocha, E. N. S. Muccillo, *J. Alloys Comp.* **400** [1-2] (2005) p. 83.

- [12] J. Yang, Z. Wen, Z. Gu, D. Yan, *J. Eur. Ceram. Soc.* **25** (2005) p. 3315.
- [13] R. Subasri, H. Nāfe, F. Aldinger, *Mater. Res. Bull.* **38** (2003) p. 1965.
- [14] R. A. Rocha, E. N. S. Muccillo, *Chem. Mater.* **15** (2003) p. 4268.
- [15] D. Marrero-López, J. C. Ruiz-Morales, P. Núñez, J. C. C. Abrantes, J. R. Frade, *J. Solid State Chem.* **177** (2004) p. 2377.
- [16] D. Marrero-López, J. Canales-Vázquez, J. C. Ruiz-Morales, A. Rodríguez, J. T. S. Irvine, P. Núñez, *Solid State Ionics* **176** (2005) p. 1807.
- [17] M. P. Pechini, *U.S. Patent 3,330,697* (1967).
- [18] S. Georges, F. Goutenoire, O. Bohnke, M. C. Steil, S. J. Skinner, H. D. Wiemhöfer, P. Lacorre, *J. New Mater. Electrochem. Systems* **7** (2004) p. 51.
- [19] F. Goutenoire, O. Isnard, E. Suard, O. Bohnke, Y. Laligant, R. Retoux, P. Lacorre, *J. Mater. Chem.* **11** (2001) p. 119.
- [20] C. Tealdi, G. Chiodelli, L. Malavasi, G. Flor, *J. Mater. Chem.* **14** (2004) p. 3553.